

THE COMPLETE CLASSIFICATION OF LARGE-AMPLITUDE GEOSTROPHIC FLOWS IN A TWO-LAYER FLUID

E. S. BENILOV¹ and G. M. REZNIK²

¹*Department of Applied Computing & Mathematics,
University of Tasmania, P.O. Box 1214, Launceston,
7250, Australia*

²*P. P. Shirshov Institute of Oceanology,
23 Krasikova St., Moscow, 117218, Russia*

(Received 22 August 1994; in final form 23 October 1995)

We examine two-layer geostrophic flows over a flat bottom on the β -plane. If the displacement of the interface is of the order of the depth of the upper layer, the dynamics of the flow depends on the following non-dimensional parameters: (i) the Rossby number ε , (ii) the ratio δ of the depth of the upper layer to the total depth of the fluid, (iii) the “ β -effect number” $\alpha = R_0/R_e \cot \theta$, where R_0 is the deformation radius, R_e is the earth’s radius and θ is the latitude. In this paper,

- 1) we derive four sets of asymptotic equations which cover the parameter space ($\varepsilon \ll 1, \alpha, \delta$).
- 2) In order to find out, which asymptotic regimes are relevant to the real ocean, we estimate ε, δ and α for a number of frontal flows in the Northern Pacific and Southern oceans.
- 3) We also discuss the stability properties of large-amplitude geostrophic flows and classify them in the $(\varepsilon, \alpha, \delta)$ -space.

KEY WORDS: β -plane, frontal flows, two-layer fluid.

1. INTRODUCTION

Consider a two-layer fluid bounded by two rigid horizontal planes. Introducing the densities $\rho_{1,2}$ of the layers (the subscript ₁ corresponds to the upper layer) and the total depth H_0 of the fluid, we define the deformation radius:

$$R_0 = \sqrt{g' H_0} / f, \quad (1.1a)$$

where $g' = g(\rho_2 - \rho_1) / \rho_2$ is the reduced acceleration due to gravity and f is the Coriolis parameter. We shall also use the deformation radius R_* based on the characteristic depth H_* of the upper (active) layer:

$$R_* = \sqrt{g' H_*} / f. \quad (1.1b)$$

The dynamics of stratified fluid on the β -plane are determined by the following non-dimensional parameters:

1) the Rossby number

$$\varepsilon = U_* / f L_*, \quad (1.2)$$

where U_* is the velocity scale and L_* is the horizontal spatial scale.

Most of the major ocean currents (except, possibly, the Gulf Stream) are geostrophic, i.e. correspond to $\varepsilon \ll 1$.

2) the β -effect number

$$\alpha = (R_0 / R_e) \cot \theta, \quad (1.3)$$

where θ is the latitude and R_e is the earth's radius [α is the ratio of the β -parameter to (f/R_0)]. As $R_0 \ll R_e$, α is always small.

3) the ratio δ of the characteristic depth of the upper layer to the total depth of the fluid

$$\delta = H_* / H_0. \quad (1.4)$$

In the real ocean, $1/2 \gtrsim \delta \gtrsim 1/15$.

4) the ratio A of the displacement of the interface to the average depth of the upper layer:

$$A = \delta H_* / H_*.$$

In some cases this parameter is small (e.g. for Rossby waves); but all oceanic frontal currents, as well as a number of other phenomena (e.g. lenses) correspond to $A \sim 1$.

Following the pioneering work of C.G. Rossby (1937), most attention in the literature focused on small-amplitude geostrophic flows, where both ε and δ are small (a review of these results can be found in any GFD monograph, e.g. Pedlosky 1987). Large-amplitude ($A \sim 1$) flows began to receive attention only in the early eighties.

Our paper is devoted to the large-amplitude geostrophic flows, i.e. flows with

$$\varepsilon \ll 1, \quad A \sim 1.$$

The examples of such are numerous in the ocean, which alone makes them worth studying. At the same time, the importance of these phenomena has been recognized a relatively short time ago and, by comparison with other areas of geophysical fluid dynamics, they attract very few investigators.

Section 2 of this paper gives a review of previous results on dynamics of large-amplitude geostrophic flows (LAGF). Section 3 presents the complete classification of LAGF in the space of parameters $(\varepsilon, \alpha, \delta)$. In Section 4 we estimate the parameters of some real-life oceanic flows and provide examples for the above classification. In Section 5 we discuss the stability properties of LAGF.

2. REVIEW OF PREVIOUS RESULTS

In this section, we shall review some of the previous work on large-amplitude (not necessarily geostrophic) flows. There have been developed three approaches to the dynamics of those.

1) The first approach is based on the direct analysis of the primitive equations of two-layer fluid dynamics. For the first time it was implemented by Orlandy (1968), who demonstrated numerically that a front of constant slope, separating two uniform layers of different densities and velocities on the f -plane ($\alpha = 0$), is unstable. Two modes of unstable perturbations were found: one, corresponding to baroclinic instability; the other, describing unstable gravity waves.

Orlandy's work was generalized for fronts of arbitrary shape (the velocity in the lower layer was still assumed uniform) by Killworth *et al.* (1984), who calculated the parameters of instability using the expansion in both small k and δ (k is the wavenumber of the perturbation and δ is the relative depth of the upper layer). They extended their analytical results numerically, for one specific front shape, to the case where the upper layer was thick ($\delta \sim 1$). Later Paldor and Killworth (1987) generalized the results of Killworth, *et al.* (1984) for double fronts (i.e. fronts for which the depth of the upper layer vanishes on both sides of the flow). Sakai (1989) and Paldor and Ghil (1990) found that an additional instability can occur for both single and double fronts in a narrow spectral interval, where the phase speeds of the baroclinic and gravity modes coalesce. Finally, Dewar and Killworth (1994) studied the stability of large-amplitude circular vortices on the f -plane.

All in all, the approach based on primitive equations proved to be very effective in stability problems for currents and vortices. However, the analytical part of the results obtained was not generalized for thick upper layer, or for the β -plane, as the zeroth-order eigenfunction used by Killworth, *et al.* (1984) is not valid for $\delta \sim 1$ or $\alpha \neq 0$. In addition, both analytical and numerical results are very difficult to generalize for continuously stratified flows, the stability equations for which are two-dimensional and elliptic.

2) The second approach to dynamics of large-amplitude flows is based on the one-layer reduced-gravity model, where the bottom layer is assumed infinitely deep. Using this model, Griffiths, *et al.* (1982) calculated the growth rate of the gravity mode for a double front, and Killworth (1983) found the necessary condition of instability for a single front (both results were obtained analytically using the long-wave expansion and then extended numerically to finite k for some specific front shapes). By comparison with the first approach, the equations of the reduced-gravity model are much simpler and allow, sometimes, to extend the analytical results to finite wavenumbers (Paldor, 1983), or consider weakly nonlinear perturbations (Paldor, 1986).

It should be noted, however, that the direct comparison of the two-layer and one-layer results (Killworth, 1983) demonstrated that the one-layer reduced gravity model requires an unrealistic restriction of the depth of the upper layer: $\delta \lesssim 0.01$. In other words, it is not applicable to the real ocean, where $1/2 \gtrsim \delta \gtrsim 1/15$.

3) The third approach to the dynamics of large-amplitude flows is based on the smallness of the Rossby number

$$\varepsilon \ll 1.$$

This condition is not very restrictive, as all of the large-scale oceanic currents (except, possibly, the Gulf Stream) are geostrophic (this question will be discussed in more detail in Section 4). In the context of large-amplitude flows this approach was

suggested by Williams and Yamagata (1984), who derived an asymptotic geostrophic equation from the one-layer reduced-gravity model. Using this equation, Cushman-Roisin (1986) constructed a solution which describes a rotating elliptical vortex and proved the stability of a wedge-like front. The latter result was generalized by Benilov (1992b), who proved the stability of all fronts with monotonic interface profiles, as well as instability of all non-monotonic fronts (Benilov, 1995a; see also Pavia, 1992).

Asymptotic equations governing two-layer LAGF were derived by Cushman-Roisin *et al.* (1992) and Benilov (1992a), and used by Benilov (1992a, 1995a) Swaters (1993) and Benilov and Cushman-Roisin (1994) in their studies of the stability of zonal flows.

By comparison with the exact two-layer equations, the geostrophic model is much simpler and therefore yields stronger results: in particular, many geostrophic results can be readily generalized for continuous stratification (Tai and Nilner, 1985; Benilov 1993, 1994, 1995b). At the same time (and in contrast to the one-layer reduced-gravity model), geostrophic approximation describes real-life oceanic currents. The only obvious shortcoming of the geostrophic approach is the impossibility of derivation of a single asymptotic system for flows with arbitrary values of the non-dimensional parameters α and δ . As a result, one has to consider several geostrophic regimes and the corresponding number of asymptotic sets of equations.

The main goal of this paper is the classification of these regimes.

3. CLASSIFICATION OF LARGE-AMPLITUDE GEOSTROPHIC FLOWS

3.1. Asymptotic analysis of the governing equations

Consider a light fluid layer on top of a heavier fluid layer. The depths $h_{1,2}$ of the layers satisfy

$$h_2 = H_0 - h_1, \quad (3.1a)$$

where H_0 is the total depth of the ocean (as we use the rigid-lid approximation, H_0 is assumed constant). The pressure p_1 in the upper layer can be expressed through h_1 and the pressure in the lower layer p_2 :

$$p_2 = p_1 - g' h_1. \quad (3.1b)$$

Then, introducing the velocities $\mathbf{u}_{1,2} = (u_{1,2}, v_{1,2})$, the horizontal spatial variables (x, y) and time t , we can write the governing equations as follows:

$$\frac{\partial \mathbf{u}_1}{\partial t} + \mathbf{u}_1 \cdot \nabla \mathbf{u}_1 + \nabla p_1 = (f + \beta y) \mathbf{u}_1 \times \mathbf{k}, \quad (3.2a)$$

$$\frac{\partial h_1}{\partial t} + \nabla \cdot (h_1 \mathbf{u}_1) = 0; \quad (3.2b)$$

$$\frac{\partial \mathbf{u}_2}{\partial t} + \mathbf{u}_2 \cdot \nabla \mathbf{u}_2 + \nabla p_2 = (f + \beta y) \mathbf{u}_2 \times \mathbf{k}, \quad (3.2c)$$

$$\frac{\partial h_2}{\partial t} + \nabla \cdot (h_2 \mathbf{u}_2) = 0, \quad (3.2d)$$

where $\mathbf{u} \times \mathbf{k} = (v, -u)$, $f = 2\Omega \sin \theta$ is the Coriolis parameter; Ω the angular frequency of the earth's rotation; θ the latitude; $\beta = (2\Omega/R_e) \cos \theta$; and R_e the earth's radius.

It is convenient to replace $\mathbf{u}_{1,2}$ by the barotropic and baroclinic components of the flow:

$$\mathbf{u}_{bt} = \frac{1}{H_0} (h_1 \mathbf{u}_1 + h_2 \mathbf{u}_2), \quad (3.3a)$$

$$\mathbf{u}_{bc} = \mathbf{u}_1 - \mathbf{u}_2. \quad (3.3b)$$

In terms of the new variables, equations (3.1, 3.2) become

$$\begin{aligned} \frac{\partial \mathbf{u}_{bt}}{\partial t} + \mathbf{u}_{bt} \cdot \nabla \mathbf{u}_{bt} + \mathbf{u}_{bc} \cdot \nabla \left[\frac{h_1(H_0 - h_1)}{H_0^2} \mathbf{u}_{bc} \right] + \frac{h_1(H_0 - h_1)}{H_0^2} \mathbf{u}_{bc} \cdot \nabla \mathbf{u}_{bc} \\ + \nabla \left(p_1 - g' h_1 + \frac{1}{2} \frac{g'}{H_0} h_1^2 \right) = (f + \beta y) \mathbf{u}_{bt} \times \mathbf{k}, \end{aligned} \quad (3.4a)$$

$$\nabla \cdot \mathbf{u}_{bt} = 0, \quad (3.4b)$$

$$\begin{aligned} \frac{\partial \mathbf{u}_{bc}}{\partial t} + \mathbf{u}_{bt} \cdot \nabla \mathbf{u}_{bc} + \mathbf{u}_{bc} \cdot \nabla \mathbf{u}_{bt} + \frac{H_0 - 2h_1}{H_0} \mathbf{u}_{bc} \cdot \nabla \mathbf{u}_{bc} - \frac{1}{H_0} \mathbf{u}_{bc} (\mathbf{u}_{bc} \cdot \nabla h_1) \\ + g' \nabla h_1 = (f + \beta y) \mathbf{u}_{bc} \times \mathbf{k}, \end{aligned} \quad (3.4c)$$

$$\frac{\partial h_1}{\partial t} + \nabla \cdot \left[h_1 \mathbf{u}_{bt} + \frac{h_1(H_0 - h_1)}{H_0} \mathbf{u}_{bc} \right] = 0. \quad (3.4d)$$

Equation (3.4b) allows one to introduce a barotropic streamfunction:

$$u_{bt} = -\frac{\partial \psi}{\partial y}, \quad v_{bt} = \frac{\partial \psi}{\partial x}. \quad (3.5)$$

Taking curl of equation (3.4a), substituting (3.5) and omitting the subscripts $_1$ and $_{bc}$, we rewrite (3.4) as follows:

$$\begin{aligned} \frac{\partial \nabla^2 \psi}{\partial t} + J(\psi, \nabla^2 \psi) \\ + \frac{\partial^2}{\partial x^2} \left[\frac{h(H_0 - h)}{H_0^2} uv \right] - \frac{\partial^2}{\partial y^2} \left[\frac{h(H_0 - h)}{H_0^2} uv \right] - \frac{\partial^2}{\partial x \partial y} \left[\frac{h(H_0 - h)}{H_0^2} (u^2 - v^2) \right] \\ + \beta \frac{\partial \psi}{\partial x} = 0, \end{aligned} \quad (3.6a)$$

$$\begin{aligned} \frac{\partial u}{\partial t} + J(\psi, u) - \left(u \frac{\partial^2 \psi}{\partial x \partial y} + \frac{\partial^2 \psi}{\partial y^2} \right) \\ + \frac{H_0 - 2h}{H_0} \left(u \frac{\partial u}{\partial x} + v \frac{\partial u}{\partial y} \right) - \frac{1}{H_0} u \left(u \frac{\partial h}{\partial x} + v \frac{\partial h}{\partial y} \right) + g' \frac{\partial h}{\partial x} = (f + \beta y) v, \end{aligned} \quad (3.6b)$$

$$\begin{aligned} \frac{\partial v}{\partial t} + J(\psi, v) - \left(u \frac{\partial^2 \psi}{\partial x^2} + v \frac{\partial^2 \psi}{\partial x \partial y} \right) \\ + \frac{H_0 - 2h}{H_0} \left(u \frac{\partial v}{\partial x} + v \frac{\partial v}{\partial y} \right) - \frac{1}{H_0} v \left(u \frac{\partial h}{\partial x} + v \frac{\partial h}{\partial y} \right) + g' \frac{\partial h}{\partial y} = -(f + \beta y)u, \end{aligned} \quad (3.6c)$$

$$\frac{\partial h}{\partial t} + J(\psi, h) + \frac{\partial}{\partial x} \left[\frac{h(H_0 - h)}{H_0} u \right] + \frac{\partial}{\partial y} \left[\frac{h(H_0 - h)}{H_0} v \right] = 0, \quad (3.6d)$$

where $J(\psi, h) = \psi_x h_y - \psi_y h_x$ is the Jacobian operator.

Next we shall scale equations (3.6):

$$\left. \begin{aligned} x &= L_* \tilde{x}, & y &= L_* \tilde{y}, & t &= T_* \tilde{t}, \\ u &= U_* \tilde{u}, & v &= U_* \tilde{v}, \\ \psi &= \Psi_* \tilde{\psi}, & h &= H_* \tilde{h}, \end{aligned} \right\} \quad (3.7a)$$

where the tildas and asterisks mark the non-dimensional variables and the corresponding characteristic scales, respectively. We shall assume that the velocity scale satisfies the geostrophic relation:

$$U = g' \delta H_* / f L_*, \quad (3.7b)$$

where δH_* is the characteristic displacement of the interface. As we are concerned with large-amplitude flows, we assume

$$\delta H_* = H_*. \quad (3.7c)$$

Substitution of (3.7) into (3.6) yields (tildas omitted)

$$\begin{aligned} \varepsilon_T \varepsilon_{bt} \frac{\partial \nabla^2 \psi}{\partial t} + \varepsilon_{bt}^2 J(\psi, \nabla^2 \psi) + \varepsilon_\beta \varepsilon_{bt} \frac{\partial \psi}{\partial x} \\ + \delta \varepsilon_{bc}^2 \left\{ \frac{\partial^2}{\partial x^2} [h(1 - \delta h)uv] - \frac{\partial^2}{\partial y^2} [h(1 - \delta h)uv] \right. \\ \left. - \frac{\partial^2}{\partial x \partial y} [h(1 - \delta h)(u^2 - v^2)] \right\} = 0 \end{aligned} \quad (3.8)$$

$$\begin{aligned} \varepsilon_T \frac{\partial u}{\partial t} + \varepsilon_{bt} \left[J(\psi, u) - \left(u \frac{\partial^2 \psi}{\partial x \partial y} + v \frac{\partial^2 \psi}{\partial y^2} \right) \right] \\ + \varepsilon_{bc} \left[(1 - 2\delta h) \left(u \frac{\partial u}{\partial x} + v \frac{\partial u}{\partial y} \right) - \delta u \left(u \frac{\partial h}{\partial x} + v \frac{\partial h}{\partial y} \right) \right] + \frac{\partial h}{\partial x} = (1 + \varepsilon_\beta y)v, \end{aligned} \quad (3.9a)$$

$$\begin{aligned} \varepsilon_T \frac{\partial v}{\partial t} + \varepsilon_{bt} \left[J(\psi, v) + \left(u \frac{\partial^2 \psi}{\partial x^2} + v \frac{\partial^2 \psi}{\partial x \partial y} \right) \right] \\ + \varepsilon_{bc} \left[(1 - 2\delta h) \left(u \frac{\partial v}{\partial x} + v \frac{\partial v}{\partial y} \right) - \delta v \left(u \frac{\partial h}{\partial x} + v \frac{\partial h}{\partial y} \right) \right] + \frac{\partial h}{\partial y} = -(1 + \varepsilon_\beta y)u, \end{aligned} \quad (3.9b)$$

$$\varepsilon_T \frac{\partial h}{\partial t} + \varepsilon_{bc} J(\psi, h) + \varepsilon_{bc} \left[\frac{\partial}{\partial x} h(1 - \delta h)u + \frac{\partial}{\partial y} h(1 - \delta h)v \right] = 0, \quad (3.10)$$

where

$$\varepsilon = U_* / fL_*, \quad (3.11)$$

$$\varepsilon_\psi = \Psi_* / fL_*^2, \quad \delta = H_* / H_0, \quad \varepsilon_T = 1 / fT_*, \quad \varepsilon_\beta = \beta L_* / f.$$

Observe that smallness of ε implies that the spatial scale of the flow is much larger than the deformation radius based on the depth of the upper layer:

$$R_* / L_* = \varepsilon^{1/2} \ll 1. \quad (3.12)$$

This equality has been obtained through substitution of (3.7b), (3.7c) and (1.1b) into (3.11).

Next, assuming that $\varepsilon_T, \varepsilon_\beta, \varepsilon_\psi$, and ε are small, we expand equations (3.9) as follows:

$$\begin{aligned} v = & \frac{\partial h}{\partial x} - \varepsilon_\beta y \frac{\partial h}{\partial x} - \varepsilon(1 - 2\delta h)J\left(h, \frac{\partial h}{\partial y}\right) - \varepsilon_T \frac{\partial^2 h}{\partial t \partial y} - \varepsilon_\psi J\left(\psi, \frac{\partial h}{\partial y}\right) \\ & + O(\varepsilon_\beta^2, \varepsilon^2, \varepsilon_T^2, \varepsilon_\psi^2, \varepsilon_\beta \varepsilon, \varepsilon_\beta \varepsilon_T, \varepsilon_\beta \varepsilon_\psi, \varepsilon \varepsilon_T, \varepsilon \varepsilon_\psi, \varepsilon_T \varepsilon_\psi), \end{aligned} \quad (3.13a)$$

$$\begin{aligned} u = & -\frac{\partial h}{\partial y} + \varepsilon_\beta y \frac{\partial h}{\partial y} - \varepsilon(1 - 2\delta h)J\left(h, \frac{\partial h}{\partial x}\right) - \varepsilon_T \frac{\partial^2 h}{\partial t \partial x} - \varepsilon_\psi J\left(\psi, \frac{\partial h}{\partial x}\right) \\ & + O(\varepsilon_\beta^2, \varepsilon^2, \varepsilon_T^2, \varepsilon_\psi^2, \varepsilon_\beta \varepsilon, \varepsilon_\beta \varepsilon_T, \varepsilon_\beta \varepsilon_\psi, \varepsilon \varepsilon_T, \varepsilon \varepsilon_\psi, \varepsilon_T \varepsilon_\psi). \end{aligned} \quad (3.13b)$$

Substituting (3.13) into (3.8) and (3.10), we rearrange the last terms in the resulting equations and obtain

$$\begin{aligned} \varepsilon_T \varepsilon_\psi \frac{\partial \nabla^2 \psi}{\partial t} + \varepsilon_\psi^2 J(\psi, \nabla^2 \psi) + \varepsilon_\beta \varepsilon_\psi \frac{\partial \psi}{\partial x} + \delta \varepsilon^2 \nabla \cdot [h(1 - \delta h)J(h, \nabla h)] \\ = O(\delta \varepsilon^2 \varepsilon_\beta, \delta \varepsilon^3, \delta \varepsilon^2 \varepsilon_\psi, \delta \varepsilon^2 \varepsilon_T), \end{aligned} \quad (3.14a)$$

$$\begin{aligned} \varepsilon_T \frac{\partial h}{\partial t} + \varepsilon_\psi J(\psi, h) - \varepsilon \varepsilon_\beta h(1 - \delta h) \frac{\partial h}{\partial x} - \varepsilon^2 \nabla \cdot [h(1 - \delta h)(1 - 2\delta h)J(h, \nabla h)] \\ = O(\varepsilon \varepsilon_\psi, \varepsilon \varepsilon_T, \varepsilon \varepsilon_\beta^2, \varepsilon^3, \varepsilon^2 \varepsilon_\beta). \end{aligned} \quad (3.14b)$$

[Observe that, in contrast to the quasigeostrophic approximation, we have omitted the $O(\varepsilon_T, \varepsilon_\psi)$ terms in (3.14).] As always, ε_T can be determined by balancing evolutionary (time-derivative) terms in the governing equations with the biggest non-evolutionary terms. It can be readily verified that no combination of the remaining independent parameters ($\varepsilon, \varepsilon_\psi, \delta, \varepsilon_\beta$) can equalize all terms in system (3.14), which means that some of the terms can be omitted. One cannot, however, derive a single “basic” set of equations (with all terms being of the same order) for all values of the small parameters: different regions of the parameters space ($\varepsilon, \varepsilon_\psi, \delta, \varepsilon_\beta$) correspond to different regimes (basic sets of equations).

Generally speaking, in order to classify the regimes in a system with more than one small parameter, the parameter space should be subdivided into regions, each of

which corresponds to a single parameter. Inside these regions, terms proportional to the other parameters can be omitted, and one obtains a set of equations for each region. Next, one considers the boundaries of the above regions (where two parameters are of equal “strength”), then the curves of intersection of these boundaries (where three parameters are of equal strength), etc. In the case of equations (3.14), however, the number of basic regimes is very large, making the analysis extremely tedious. Accordingly, we shall discuss only the highest-level regimes, i.e. those that include as many small parameters as possible and correspond to *points* in the parameter space. These regimes include all low-level regimes as limiting cases; at the same time, the corresponding sets of equations are still simpler than the original system (3.14) (recall that the latter is not a basic set and therefore contains terms of different orders).

Omitting (straightforward) calculations, we obtain four basic sets of equations:

$$\delta = 1, \quad \varepsilon_\beta = \varepsilon_\psi = \varepsilon \quad (\varepsilon_T = \varepsilon): \quad (3.15)$$

$$\left. \begin{aligned} \frac{\partial \nabla^2 \psi}{\partial t} + J(\psi, \nabla^2 \psi) + \frac{\partial \psi}{\partial x} + \nabla \cdot [h(1-h)J(h, \nabla h)] &= O(\varepsilon), \\ \frac{\partial h}{\partial t} + J(\psi, h) &= O(\varepsilon); \end{aligned} \right\} \quad (3.15b)$$

$$\delta = 1, \quad \varepsilon_\beta = \varepsilon^{1/2}, \quad \varepsilon_\psi = \varepsilon^{3/2} \quad (\varepsilon_T = \varepsilon^{3/2}): \quad (3.16a)$$

$$\left. \begin{aligned} \frac{\partial \psi}{\partial x} + \nabla \cdot [h(1-h)J(h, \nabla h)] &= O(\varepsilon^{1/2}), \\ \frac{\partial h}{\partial t} + J(\psi, h) - h(1-h)\frac{\partial h}{\partial x} &= O(\varepsilon^{1/2}); \end{aligned} \right\} \quad (3.16b)$$

$$\delta = \varepsilon, \quad \varepsilon_\beta = \varepsilon, \quad \varepsilon_\psi = \varepsilon^2 \quad (\varepsilon_T = \varepsilon^2): \quad (3.17a)$$

$$\left. \begin{aligned} \frac{\partial \psi}{\partial x} + \nabla \cdot [hJ(h, \nabla h)] &= O(\varepsilon), \\ \frac{\partial h}{\partial t} + J(\psi, h) - h\frac{\partial h}{\partial x} - \nabla \cdot [hJ(h, \nabla h)] &= O(\varepsilon); \end{aligned} \right\} \quad (3.17b)$$

$$\delta = \varepsilon^2, \quad \varepsilon_\beta = \varepsilon^2, \quad \varepsilon_\psi = \varepsilon^2 \quad (\varepsilon_T = \varepsilon^2): \quad (3.18a)$$

$$\left. \begin{aligned} \frac{\partial \nabla^2 \psi}{\partial t} + J(\psi, \nabla^2 \psi) + \frac{\partial \psi}{\partial x} + \nabla \cdot [hJ(h, \nabla h)] &= O(\varepsilon^2), \\ \frac{\partial h}{\partial t} + J(\psi, h) - h\frac{\partial h}{\partial x} - \nabla \cdot [hJ(h, \nabla h)] &= O(\varepsilon). \end{aligned} \right\} \quad (3.18b)$$

Systems (3.15b)–(3.18b) cover all of the parameter space of the original equations (3.14). No combination of $\varepsilon, \varepsilon_\beta, \delta$ and ε_ψ gives a system that is not included in (3.15b)–(3.18b) as a limiting case.

3.2. Discussion

(i) It is convenient to rewrite the equations derived in non-scaled non-dimensional variables determined by measurable parameters. Substituting

$$L_* = R_0, \quad T_* = f^{-1}, \quad H_* = H_0, \quad \Psi_* = R_0^2 f$$

into (3.7):

$$\left. \begin{aligned} x &= R_0 \tilde{x}, & y &= R_0 \tilde{y}, & t &= f^{-1} \tilde{t}, \\ \psi &= R_0^2 f \tilde{\psi}, & h &= H_0 \tilde{h}; \end{aligned} \right\} \quad (3.19)$$

we rewrite (3.15b)–(3.18b) as follows (tildas and small terms omitted):

$$\left. \begin{aligned} \nabla^2 \psi_t + J(\psi, \nabla^2 \psi) + \alpha \psi_x + \nabla \cdot [h(1-h)J(h, \nabla h)] &= 0, \\ h_t + J(\psi, h) &= 0; \end{aligned} \right\} \quad (3.20)$$

$$\left. \begin{aligned} \alpha \psi_x + \nabla \cdot [h(1-h)J(h, \nabla h)] &= 0, \\ h_t + J(\psi, h) - \alpha h(1-h)h_x &= 0; \end{aligned} \right\} \quad (3.21)$$

$$\left. \begin{aligned} \alpha \psi_x + \nabla \cdot [hJ(h, \nabla h)] &= 0, \\ h_t + J(\psi, h) - \alpha h h_x - \nabla \cdot [hJ(h, \nabla h)] &= 0; \end{aligned} \right\} \quad (3.22)$$

$$\left. \begin{aligned} \nabla^2 \psi_t + J(\psi, \nabla^2 \psi) + \alpha \psi_x + \nabla \cdot [hJ(h, \nabla h)] &= 0, \\ h_t + J(\psi, h) - \nabla \cdot [hJ(h, \nabla h)] &= 0, \end{aligned} \right\} \quad (3.23)$$

where the subscripts denote differentiation and α is defined by equality (1.3). In what follows, Systems (3.20) and (3.23) will be referred to as the “regimes with weak β -effect” (observe that, in these cases, the β -effect influences only the barotropic mode). The remaining systems, (3.21) and (3.22), will be referred to as the “regimes with strong β -effect”.

(ii) Note that, for all regimes (3.15a)–(3.18a), the amplitude of the barotropic mode does not exceed that of the baroclinic mode:

$$\varepsilon_\psi \lesssim \varepsilon.$$

Thus, the global Rossby number $\max\{\varepsilon_\psi, \varepsilon\}$ can be assumed to coincide with ε . This, of course, does not mean that the barotropic mode never dominates the baroclinic mode, but indicates that the barotropic regime is not a higher-order basic set and can be included in a more general set of equations [specifically, in (3.20) or (3.23)].

(iii) It is convenient to express ε_β through α . Rewriting (1.3) as follows:

$$\alpha = (R_0/R_e) \cot \theta = \beta R_0/f = \varepsilon_\beta R_0/L_* = \varepsilon_\beta (R_*/L_*)(R_0/R_*),$$

and using formulae (3.12) and (1.1a, b), we obtain

$$\alpha = \varepsilon_\beta \varepsilon^{1/2} \delta^{-1/2}.$$

Now, regimes (3.20)–(3.23) can be classified on the $(\delta/\varepsilon, \alpha/\varepsilon)$ -plane (see Table 1). Systems (3.20) and (3.21) were derived by Benilov (1992a) whereas (3.22) and (3.23) were derived (as a single system for all four bottom cells in Table 1) by Cushman Roisin *et al.* (1992). Later (3.22) and (3.23) were derived exactly in their present form by Benilov and Cushman-Roisin (1994), and Swaters (1993), respectively. Swaters’ paper also contained a generalization of (3.23) for a sloped bottom.

(iv) The scaling of equations (3.20)–(3.23) is illustrated by Table 2.

This table is particularly helpful for generalization of the results for the case of continuous stratification (which has the same scaling).

Table 1 Classification of the asymptotic regimes on the $(\alpha/\varepsilon, \delta/\varepsilon)$ -plane. ε, α and δ are defined by (1.2)–(1.4), respectively.

	<i>Weak β-effect</i> $\alpha \sim \varepsilon^{3/2}$	<i>Strong β-effect</i> $\alpha \sim \varepsilon$
$\delta \sim 1$	Regime 1, (3.20)	Regime 2, (3.21)
$\delta \sim \varepsilon$		Regime 3, (3.22)
$\delta \sim \varepsilon^2$	Regime 4, (3.23)	

Table 2 Scaling of equations (3.20)–(3.23).
 ε, α and δ are defined by (1.2)–(1.4), respectively.
 L_* is the horizontal spatial scale,
 U_{1*} and U_{2*} are the effective velocity scales,
 T_{*}^{1*} and T_{*}^{2*} are the effective time scales.

	<i>Regime number</i>	δ	α	$\frac{U_{1*}}{fR_d}$	$\frac{U_{2*}}{fR_d}$	$\frac{L_*}{R_d}$	$T_* f$
(3.20)	1	1	$\varepsilon^{3/2}$	$\varepsilon^{1/2}$	$\varepsilon^{1/2}$	$\varepsilon^{-1/2}$	ε^{-1}
(3.21)	2	1	ε	$\varepsilon^{1/2}$	$\varepsilon^{1/2}$	$\varepsilon^{-1/2}$	ε^{-2}
(3.22)	3	ε	ε	ε	ε^2	1	ε^{-2}
(3.23)	4	ε^2	$\varepsilon^{3/2}$	$\varepsilon^{3/2}$	$\varepsilon^{5/2}$	$\varepsilon^{1/2}$	ε^{-2}

(v) In order to clarify the correspondence between large- and small-amplitude geostrophic flows, we shall calculate the dispersion relations of harmonic oscillations described by (3.20)–(3.23). Substituting the harmonic-wave solution

$$h = \bar{h}_0 + h' \exp(i\omega t - imx - iny), \quad \psi = \psi' \exp(i\omega t - imx - iny)$$

(where \bar{h}_0 is the average depth of the upper layer) and neglecting nonlinear terms, we obtain

$$\left. \begin{aligned} (3.20): \quad \omega_{(3.20)} &= -\frac{\alpha m}{m^2 + n^2}, \\ (3.21): \quad \omega_{(3.21)} &= -\bar{h}_0(1 - \bar{h}_0)m, \\ (3.22): \quad \omega_{(3.22)} &= -\bar{h}_0 m, \\ (3.23) \quad \omega_{(3.23)} &= -\frac{\alpha m}{m^2 + n^2}. \end{aligned} \right\} \quad (3.24)$$

If we compare (3.24) with the standard (non-dimensional) dispersion relations of the two-layer Rossby waves:

$$\omega_{bt} = -\frac{\alpha m}{m^2 + n^2}, \quad \omega_{bc} = -\frac{\alpha m}{m^2 + n^2 + [\bar{h}_0(1 - \bar{h}_0)]^{-1}}; \quad (3.25)$$

we observe that (3.20) and (3.23) describe the barotropic mode:

$$\omega_{(3.20)} = \omega_{(3.23)} = \omega_{bt},$$

(3.21) describes the long-wave limit of the baroclinic mode:

$$\omega_{(3.21)} \approx \omega_{bc} \quad \text{if} \quad m^2 + n^2 \ll [\bar{h}_0(1 - \bar{h}_0)]^{-1},$$

and (3.22) describes the (long-wave + thin-upper-layer) limit of the baroclinic mode:

$$\omega_{(3.22)} \approx \omega_{bc} \quad \text{if} \quad m^2 + n^2 \ll [\bar{h}_0(1 - \bar{h}_0)]^{-1} \quad \text{and} \quad \bar{h}_0 \ll 1.$$

Observe that none of the systems describes both modes, the reason of which is separation of the modes' time scales. Indeed, if we substitute

$$m, n \sim \frac{R_0}{L_*}$$

(with L_* given by Table 2) into the dispersion relations (3.25), we get

$$\left. \begin{array}{ll} \text{Regime 1:} & \omega_{bt} \sim \varepsilon, \quad \omega_{bc} \sim \varepsilon^2; \\ \text{Regime 2:} & \omega_{bt} \sim \varepsilon^{1/2}, \quad \omega_{bc} \sim \varepsilon^{3/2}; \\ \text{Regime 3:} & \omega_{bt} \sim \varepsilon, \quad \omega_{bc} \sim \varepsilon^2; \\ \text{Regime 4:} & \omega_{bt} \sim \varepsilon^2, \quad \omega_{bc} \sim \varepsilon^3. \end{array} \right\} \quad (3.26)$$

These estimates show that a single-scale asymptotic expansion cannot take into account both Rossby-wave modes.

(vi) Estimates (3.26) also demonstrate that the barotropic effects in large-amplitude geostrophic dynamics are always stronger (faster) than the baroclinic effects. Generally speaking, this means that the latter should be omitted from a leading-order asymptotic equation. However, (3.21) and (3.22) do describe the baroclinic mode. This occurs because the barotropic component of the flow in these regimes is weak. In Regime 3, this is a result of the smallness of the depth the active layer; in Regime 2, it is the result of the constraint of the allowed initial conditions imposed by

$$\psi = 0. \quad (3.27)$$

Indeed, substituting (3.27) into (3.3a) and (3.5), we get

$$h_1 \mathbf{u}_1 + h_2 \mathbf{u}_2 = 0.$$

which indicates that we consider almost compensated flows. However, the barotropic mode cannot be filtered out completely, as it is generated nonlinearly by the baroclinic mode (see the first equations in Systems (3.21) and (3.22), which can be interpreted as a sort of Sverdrup's relation).

It should also be mentioned that the weak- β -effect equations (3.21) and (3.22) restrict the initial condition for the barotropic component of the flow. This can be accounted for by the above-mentioned difference in the barotropic/baroclinic time-scales, suggesting that barotropic waves rapidly disperse, after which the barotropic mode becomes enslaved by the baroclinic mode. It may occur, however, that barot-

ropic mode takes on a coherent stationary structure—a zonal flow or a stationary modon. The former case is clearly included in (3.21) and (3.22) [which are invariant with respect to adding an arbitrary zonal flow: $\psi(z,y,t) \rightarrow \psi(z,y,t) + \psi_0(y)$]. In the latter case, strong barotropic mode takes over the evolution of the interface from the baroclinic mode—such motion can be described by

$$\left. \begin{aligned} \nabla^2 \psi_t + J(\psi, \nabla^2 \psi) + \alpha \psi_x &= 0, \\ h_t + J(\psi, h) &= 0 \end{aligned} \right\}$$

(see Dewar and Gaillard 1993). Observe that this system does not make a new regime as it is included, as a limiting case, in (3.20) and (3.23).

4. APPLICABILITY OF EQUATIONS (3.20–3.23) TO THE REAL OCEAN

In order to clarify which of the equations derived are relevant to the real ocean, we shall estimate ε , δ and α for a number of real-life frontal flows. Specifically, we shall use

–Roden’s (1975) observations of the Kuroshio, Oyashio, subtropical and subarctic fronts in the Northern Pacific;

–Nowlin and Klinck’s (1986) observations of the Antarctic Circumpolar Current.

At the location where Roden’s measurements were made, the subtropical front could be subdivided into three separate jets (their axes located at $27^\circ 30'N$, $28^\circ 45'$ and $31^\circ 30'$). Nowlin and Klinck’s data indicate that the ACC in Drake’s Passage can also be subdivided into three jets (their axes located at $57^\circ 00'S$, $59^\circ 00'S$ and $51^\circ 30'S$). The parameters of all these jets will be estimated separately. In what follows, we shall use the following notation:

- K = Kuroshio;
- O = Oyashio
- SA = subarctic front;
- ST₁ = subtropical front, northern jet;
- ST₂ = subtropical front, middle jet;
- ST₃ = subtropical front, southern jet;
- ACC₁ = ACC, northern jet;
- ACC₂ = ACC, middle jet;
- ACC₃ = ACC, southern jet.

In order to make sure that we deal with large-amplitude geostrophic flows, we shall estimate maximum velocity and the effective displacement of isopycnal surfaces (see Table 3a).

This table shows that all of the above frontal flows are geostrophic ($\varepsilon_{\max} \ll 1$) and most of them (except, possibly, ST₂ and ACC₃) are of large amplitude ($A \sim 1$).

Table 3a Parameters of frontal flows in the Northern Pacific and Southern oceans.

u_{\max} is the maximum velocity,
 $2L$ is the width of the flow,
 ϵ_{\max} is the Rossby number based on U_{\max} ,
 H_* is the effective depth of the upper layer,
 δH_* is the effective displacement of isopycnal surfaces,
 $A = \delta H_*/H_*$.

	K	O	SA	ST_1	ST_2	ST_3	ACC_1	ACC_2	ACC_3
u_{\max} (m/s)	0.55	0.25	0.40	0.20	0.15	0.45	0.20	0.30	0.20
$2L$ (km)	145	100	200	210	120	150	190	130	80
ϵ_{\max}	0.085	0.054	0.042	0.026	0.035	0.089	0.017	0.037	0.039
H_* (m)	600	400	500	350	350	500	1,600	2,000	1,800
δH_* (m)	200	160	300	140	60	140	500	500	300
A	0.33	0.40	0.60	0.40	0.17	0.28	0.31	0.25	0.17

Table 3b Parameters of frontal flows in the Northern Pacific and Southern oceans.

U_{1*} is the effective velocity scale in the upper layer,
 $\frac{\Delta\rho}{\rho_0}$ is the relative density variation,
 ϵ is the Rossby number based on U_{1*} ,
 $\delta = H_*/H_0$,
 α is given by formula (1.3).

	K	O	SA	ST_1	ST_2	ST_3	ACC_1	ACC_2	ACC_3
U_{1*} (m/s)	0.26	0.12	0.20	0.12	0.09	0.25	0.13	0.18	0.12
$\frac{\Delta\rho}{\rho_0} \times 10^4$	17	7	13	13	13	18	6	5	4
H_0 (m)	5,500	5,500	5,500	5,500	5,500	5,500	4,000	4,000	3,500
ϵ	0.040	0.026	0.021	0.016	0.021	0.050	0.011	0.022	0.023
δ	0.109	0.073	0.091	0.064	0.064	0.091	0.400	0.500	0.514
α	0.021	0.012	0.015	0.031	0.034	0.044	0.004	0.004	0.002

Next we calculate ϵ , δ and α (see Table 3b) and then classify the above frontal flows on the $(\delta/\epsilon, \alpha/\epsilon)$ -plane.

Table 4 shows that Regime 4 is not relevant to any real-life fronts. Indeed, given that $\epsilon \leq 0.1$, the condition $\delta \sim \epsilon^2$ entails the unrealistic estimate $\delta \leq 0.01$ (while in the ocean $1/2 \gtrsim \delta \gtrsim 1/15$). The only possible application of the regimes with $\delta \sim \epsilon^2$ seems to be the oceanic mixed layer, whose depth varies between 50 and 150 metres. The situation with the other gap in Table 4 (thin upper layer, weak β -effect) is unclear: none of the examples fell into that cell, but this regime does not seem to be impossible in principle.

Table 4 Classification of frontal flows in the Northern Pacific and Southern Oceans.

	<i>Weak β-effect</i> $\alpha \sim \varepsilon^{3/2}$	<i>Strong β-effect</i> $\alpha \sim \varepsilon$
$\delta \sim 1$	Regime 1: ACC ₂₋₃	Regime 2: ACC ₁
$\delta \sim \varepsilon$		Regime 3: K, O, SA, ST ₁₋₃
$\delta \sim \varepsilon^2$	Regime 4: none	

5. STABILITY OF ZONAL FLOWS

In terms of the two-layer model, an isolated zonal flow with both horizontal and vertical shear is described by

$$h = \bar{h}(y), \quad \psi = - \int \bar{u}(y) dy, \quad (5.1a)$$

$$\bar{h}_y(\pm \infty) = 0, \quad \bar{u}(\pm \infty) = 0. \quad (5.1b)$$

In this section, we shall discuss the stability properties of solution (5.1) and their impact on the applicability of the equations derived. We shall distinguish two types of instability:

instability with respect to disturbances, whose length is comparable to, or longer than the width of the flow (long-wave instability),

instability with respect to disturbances, whose length is much shorter than the width of the flow (short-wave instability).

5.1. Long-wave instability

Long-wave stability of solution (5.1) can be studied within the framework of equations (3.20)–(3.23). The results obtained so far are summarized in Table 5.

These stability theorems were proven by Benilov (1992a) (Regimes 1, 2), Benilov and Cushman-Roisin (1994) (Regime 3) and Swaters (1993) (Regime 4). Finally, Benilov (1995a) argued that those Regime-3 flows, that do not satisfy the above conditions of stability, are unstable.

It should be emphasized, however, that equations (3.20)–(3.23) describe short-wave disturbances incorrectly [see restriction (3.12)]. As a result,

i) the growth rate of unstable perturbations described by (3.20) blows up in the short-wave region (Tai and Niiler, 1985; Benilov, 1992a; Young and Chen, 1994):

$$\text{Im}\omega(k) \rightarrow \infty \quad \text{as } k \rightarrow \infty,$$

where ω and k are frequency and wavenumber of disturbances, respectively. The short-wave blow-up of the instability makes numerical simulation of equation (3.20) impossible; however, (3.20) can still be used in a theoretical study, provided the physical meaning of this property is clarified.

Table 5 Long-wave stability of large-amplitude geostrophic flows.

	<i>Weak β-effect</i> $\alpha \sim \varepsilon^{3/2}$	<i>Strong β-effect</i> $\alpha \sim \varepsilon$
$\delta \sim 1$	Regime 1: instability	Regime 2: stability
$\delta \sim \varepsilon$		Regime 3: stability if $\bar{h}_y \geq 0$ or $0 \geq \bar{h}_y \geq -\alpha$
$\delta \sim \varepsilon^2$	Regime 4: stability if $\bar{h}_y \geq \max(0, \bar{u}_{yy} - \alpha)$ or $0 \geq \bar{h}_y \geq \bar{u}_{yy} - \alpha$	

ii) On the other hand, short disturbances may destabilize some of the flows, which are stable within the framework of (3.20)–(3.23).

5.2. *Short-wave instability*

First, we observe that, if the wavelength of a disturbance is much smaller than the effective spatial scale of the mean flow the stability analysis can be carried out locally in the approximation of small-amplitude geostrophic flows. Indeed, variations of the mean flow’s parameters over the wavelength of a *short* perturbation are much smaller than their average (local) values. Accordingly, we can make use of Phillips’ (1954) model, whose non-dimensional dispersion relation (e.g. Pedlosky, 1987) is:

$$c = U_2 + \frac{\bar{h}_0(1 - \bar{h}_0)Uk^4 + 2\bar{h}_0[U - (1 - \bar{h}_0)\alpha]k^2 - \alpha}{2[\bar{h}_0(1 - \bar{h}_0)k^4 + k^2]} \pm \frac{\{U^2\bar{h}_0^2(1 - \bar{h}_0)^2k^8 - 2\bar{h}_0(1 - \bar{h}_0)U[2U - (1 - 2\bar{h}_0)\alpha]k^4 + \alpha^2\}^{1/2}}{2[\bar{h}_0(1 - \bar{h}_0)k^4 + k^2]}, \quad (5.2)$$

where $U_{1,2}$ are the velocities in the layers, $U = U_1 - U_2$ and $c = \omega/k$. Assuming for simplicity that

$$\bar{h}_0 \leq \frac{1}{2},$$

one can obtain the following criterion of stability:

$$-\alpha\bar{h}_0 \leq U \leq \alpha(1 - \bar{h}_0). \quad (5.3)$$

If this condition does not hold, the spectral range of unstable disturbances is bounded by

$$K_- < k < K_+,$$

where

$$K_{\pm} = \left[\frac{2U - \alpha(1 - 2\bar{h}_0) \pm 2\sqrt{(U + \alpha\bar{h}_0)[U - \alpha(1 - \bar{h}_0)]}}{\bar{h}_0(1 - \bar{h}_0)U} \right]^{1/4} \quad (5.4)$$

Now, scaling (5.3) in accordance with Table 2:

$$\text{Regime 1: } U \rightarrow \varepsilon^{1/2} U, \quad \bar{h}_0 \rightarrow \bar{h}_0, \quad \alpha \rightarrow \varepsilon^{3/2} \alpha;$$

$$\text{Regime 2: } U \rightarrow \varepsilon^{1/2} U, \quad \bar{h}_0 \rightarrow \bar{h}_0, \quad \alpha \rightarrow \varepsilon \alpha;$$

$$\text{Regime 3: } U \rightarrow \varepsilon U, \quad \bar{h}_0 \rightarrow \varepsilon \bar{h}_0, \quad \alpha \rightarrow \varepsilon \alpha;$$

$$\text{Regime 4: } U \rightarrow \varepsilon^{3/2} U, \quad \bar{h}_0 \rightarrow \varepsilon^2 \bar{h}_0, \quad \alpha \rightarrow \varepsilon^{3/2} \alpha;$$

and then taking the limit $\varepsilon \rightarrow 0$, we obtain

$$\text{Regime 1: instability;} \tag{5.5a}$$

$$\text{Regime 2: instability;} \tag{5.5b}$$

$$\text{Regime 3: stability if } 0 \lesssim U \lesssim \alpha, \text{ instability otherwise;} \tag{5.5c}$$

$$\text{Regime 4: stability if } 0 \lesssim U \lesssim \alpha, \text{ instability otherwise;} \tag{5.5d}$$

Scaling of (5.4), in turn, yields

$$\text{Regime 1: } K_- \sim \varepsilon^{1/2}, \quad K_+ \sim 1;$$

$$\text{Regime 2: } K_- \sim \varepsilon^{1/4}, \quad K_+ \sim 1;$$

$$\text{Regime 3: } K_- \sim \varepsilon^{-1/4}, \quad K_+ \sim \varepsilon^{-1/4};$$

$$\text{Regime 4: } K_- \sim \varepsilon^{-1/2}, \quad K_+ \sim \varepsilon^{-1/2}.$$

Comparing these estimates with the spatial scale of equations (3.20)–(3.23) (see Table 2, $K \sim L_*^{-1}$):

$$(3.20): \quad K \sim \varepsilon^{1/2},$$

$$(3.21): \quad K \sim \varepsilon^{1/2},$$

$$(3.22): \quad K \sim 1,$$

$$(3.23): \quad K \sim \varepsilon^{-1/2};$$

we can draw the following conclusions:

i) Equation (3.20) does not describe the short-wave cutoff K_+ because the latter is inconsistent with its scaling.

The long-wave cutoff K_- is consistent with the scaling of (3.20), hence the wavelength of unstable disturbances can be comparable to the width of the mean flow. Generally speaking, this means that the local approximation used in deriving (5.3)–(5.4) does not hold and the results obtained should be verified using (3.20).

ii) For Regime 2, both cutoffs are inconsistent with the scaling of system (3.21). All unstable disturbances are much shorter than the width of the mean flow, which is why (3.21) does not describe instability at all (it has been scaled out). It may be conjectured, however, that the short-wave instability is unlikely to destroy the flow, but leads to randomization of unstable disturbances, and the resulting turbulent friction may stabilize the flow. This conclusion applies only to the short-wave instability, while a long-wave instability usually results in meandering of the mean flow, which can break it up completely.

iii) For Regime 3, both cutoffs are inconsistent with the scaling of the corresponding asymptotic system, but, in contrast to Regime 2, the short-wave instability does

not take place in all cases. In order to compare the short-wave results (5.5) with the long-wave results in Table 5 and determine a region of overall stability (if any), we should relate U to \bar{h} :

$$U = -\bar{h}_y,$$

after which the criterion of short-wave stability (5.5c) becomes

$$\text{Regime 3: stability, if } 0 \leq -\bar{h}_y \leq \alpha, \text{ otherwise instability.} \tag{5.6}$$

Thus, short-wave instability eliminates one of the two cases of (otherwise stable) Regime-3 flows (Benilov and Cushman-Roisin, 1994).

iv) For Regime 4, K_{\pm} are both consistent with the scaling of system (3.23), which means that an instability (if any) occurs in the long-wave region and is described by (3.23). Result (5.5d) obtained via (invalid) local approximation is apparently incorrect. Thus we conclude that, in this regime, zonal flows are stable with respect to short perturbations.

The above results on short-wave instability of large-amplitude geostrophic flows are summarized in Table 6:

Using data in Table 3a, one can estimate the slope of the interface \bar{h}_y for the North Pacific frontal system and ACC, and hence calculate the parameters of their instability (see Table 7).

The Oyashio frontal flow is not zonal, hence criterion (5.6) is inapplicable.

Table 7 demonstrates that wavelengths of unstable perturbations are comparable to the width of the mean flow (compare λ_{\max} and $\lambda_{1,2}$ with $2L$ from Table 3a). This means that the local approximation is only of limited relevance to the real ocean, and that results in Table 7 should be treated as rough estimates. However, a certain tendency can be observed: instability of flows with thick upper layer takes place in a wider spectral range than that of flows with thin upper layer.

5.3. Discussion

i) It is worth noting that both weak- β -effect systems admit the following steady solution

$$h = \bar{h} [(\cos \phi) x + (\sin \phi) y], \quad \psi = 0;$$

Table 6 Short-wave stability of large-amplitude geostrophic flows.

	<i>Weak β-effect</i> $\alpha \sim \varepsilon^{3/2}$	<i>Strong β-effect</i> $\alpha \sim \varepsilon$
$\delta \sim 1$	Regime 1: instability	Regime 2: instability
$\delta \sim \varepsilon$		Regime 3: stability if $0 \leq \bar{h}_y \leq -\alpha$, instability otherwise
$\delta \sim \varepsilon^2$	Regime 4: stability	

Table 7 Short-wave instability of frontal flows in the Northern Pacific and Southern oceans.

$\bar{h}_y = \frac{\delta H_* / H_0}{L_* / R_d}$ is the slope of the interface;

α is the β -effect number (if $\bar{h}_y + \alpha > 0$, the flow is stable);

$\lambda_{1,2}$ = half-lengths of the marginally stable disturbances;

λ_{\max} = half-length of the fastest growing disturbance;

τ = time of the fastest growth.

	<i>Regime</i>	\bar{h}_y	α	$\tau(\text{days})$	$\lambda_{\max}(\text{km})$	$\lambda_1(\text{km})$	$\lambda_2(\text{km})$
K	3	-0.027	0.021	18	190	160	265
SA	3	-0.024	0.015	16	150	120	235
ST ₁	3	-0.014	0.031		stable		
ST ₂	3	0.011	0.034	22	130	110	185
ST ₃	3	-0.025	0.044		stable		
ACC ₁	2	-0.026	0.004	9	95	60	315
ACC ₂	1	-0.037	0.004	6	95	60	370
ACC ₃	1	-0.031	0.002	7	70	45	360

which describes a non-zonal flow (ϕ is the angle between the direction of the flow and the x -axes). This flow does not transfer mass across the β -plane ($\psi = 0$), i.e. the current in the upper layer is compensated by the counter-current in the lower layer (see Benilov, 1992a). The stability properties of this solution have not yet been examined.

ii) It has been demonstrated that system (3.20) does not describe the shortwave cutoff of baroclinic instability. In order to demonstrate that it describes at least the long-wave cutoff (which is consistent with its scaling), we applied (3.20) to a small-amplitude flow and compared the results with the traditional quasigeostrophic approximation. We considered the simplest particular case of (5.1):

$$\bar{h}(y) = \bar{h}_0 + \gamma y, \quad \bar{u}(y) = \bar{u}_0 \quad (5.7a)$$

in a zonal channel:

$$-\frac{1}{2}\ell < y < \frac{1}{2}\ell \quad (5.7b)$$

and assumed that the displacement of the interface is small:

$$\gamma\ell \ll 1.$$

Straightforward calculation demonstrated that the dispersion relation of disturbances governed by (3.20) coincide with the quasigeostrophic relation (5.2) if

$$k^2 \ll \frac{1}{\bar{h}_0(1 - \bar{h}_0)}, \quad \alpha \ll |\gamma|$$

(see Figure 1). these conditions confirm that system (3.20) describes long waves with an additional assumption of weakness of the β -effect.

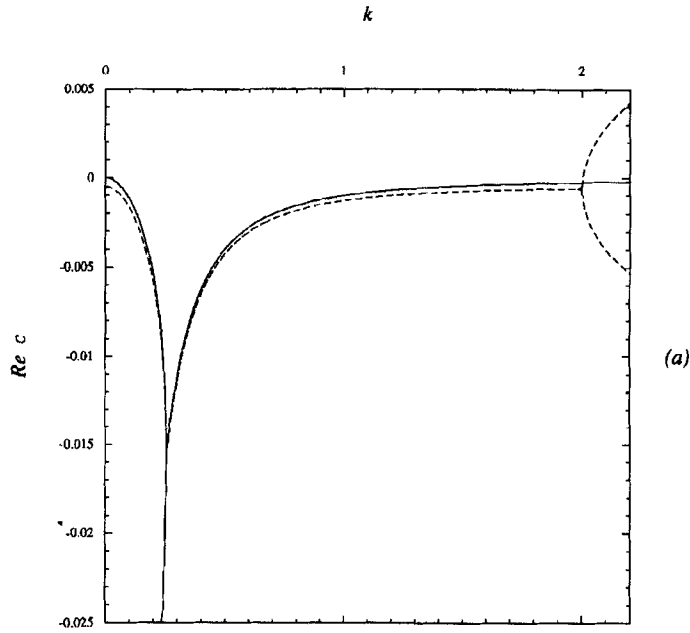


Figure 1a

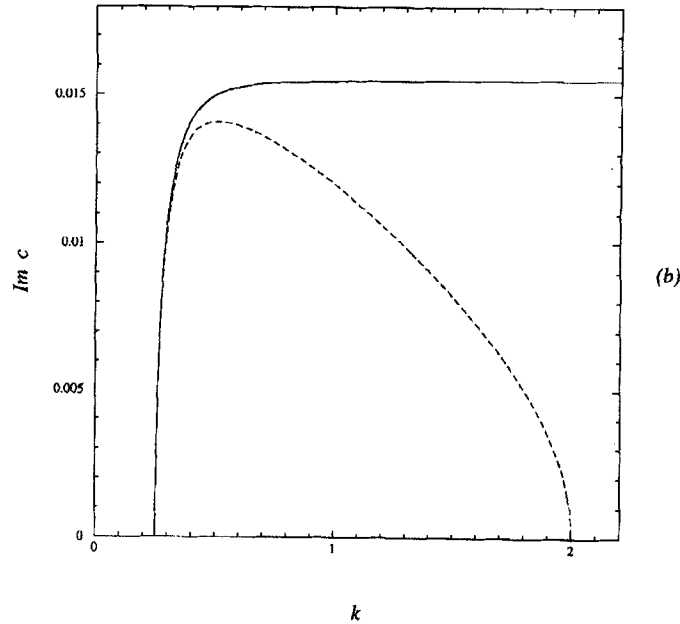


Figure 1 The dispersion relation of baroclinic instability. Parameters correspond to the southern jet of the Antarctic Circumpolar Current (ACC₃): $\bar{h}_0 = 0.514$, $\gamma = U = 0.031$, $\alpha = 0.002$, $\bar{u} = 0$. (a) $Re\ c$ vs k , (b) $Im\ c$ vs k . c and k are the phase speed and wavenumber of disturbances, respectively. Solid line represents the dispersion relation calculated using system (3.20), Dashed line represents quasigeostrophic approximation (5.2).

iii) It should be noted that, as a result of the short-wave blow-up, system (3.20) describes only the initial stage of baroclinic instability. Indeed, even if the initial condition consists of only long disturbances, nonlinear interaction generates short waves and (3.20) fails!

However, if we are prepared to sacrifice simplicity, it is possible to derive a system, which describes both short and long disturbances. To do so, we should take into account the (higher-order) $O(\varepsilon_T, \varepsilon_\psi)$ terms in equations (3.14). Omitting calculations and writing the resulting equations in the non-scaled non-dimensional variables (3.19), we have

$$\nabla^2 \psi_t + J(\psi, \nabla^2 \psi) + \nabla \cdot [h(1-h)J(h, \nabla h)] + \alpha \psi_x = 0; \quad (5.8a)$$

$$h_t + J(\psi, h) - \alpha h(1-h)h_x - \nabla \cdot \{h[(1-h)(1-2h)J(h, \nabla h) + \nabla h_t + J(\psi, \nabla h)]\} = 0. \quad (5.8b)$$

For long disturbances, the new terms do not contribute to the accuracy of system (5.8). For short disturbances, however, the new terms are of the same order as the main terms in equation (5.8b). One can readily derive from (5.8) the standard two-layer quasigeostrophic equations.

Finally, we note that (5.8) includes all four large-amplitude regimes as limiting cases and describes small-amplitude (quasigeostrophic) motion as well. Systems similar to (5.8) were derived by Benilov (1992a) and Young (1994), but, although their equations do have short-wave cutoffs of baroclinic instability (which is qualitatively correct), they do not provide quantitative description of short disturbances. A quantitatively correct system for flows with thin upper layer was derived by Cushman-Roisin *et al.* (1992).

6. CONCLUSIONS

In this section, we shall summarize the main results of this paper.

Firstly, we have presented the complete classification of large-amplitude geostrophic regimes in the space of parameters $\varepsilon \ll 1$, α and δ [defined by (1.2)–(1.4), respectively]; and derived four systems of equations that correspond to the basic regimes [see Table 1 and equations (3.20)–(3.23)]. The equations governing these regimes

- include as many terms as possible provided these terms are of the same order
- and include all other regimes as limiting cases (i.e. cover all of the parameter space).

The criterion of applicability of the equations derived is

$$(R_*/L_*)^2 \ll 1, \quad (6.1)$$

Where L_* is the horizontal scale of the motion and R_* is given by (1.1b).

It turned out, however, that some of sets (3.20–3.23) are not self-contained, i.e. drive the solution outside of their applicability regions [see Section 5.3 (iii)]. Hoping that the solution remains, at least, geostrophic, we constructed a more complicated set of equations, which describe all possible regimes of large-amplitude geostrophic

flows and small-amplitude (quasigeostrophic) motion as well [equations (5.8)]. This system can be used in numerical modeling of oceanic frontal currents: with (fast) gravity waves scaled out, it must have less numerical instabilities than the primitive equations. The criterion of its applicability is

$$\varepsilon \ll 1, \quad (6.2)$$

where ε is the Rossby number. If the initial condition includes small-amplitude short disturbances, restriction (6.2) is weaker than (6.1) (small-amplitude disturbances do not have to be long to be geostrophic).

Secondly, we have classified previous results on the stability of large-amplitude geostrophic zonal flows and filled out the gaps in this classification (Tables 5–6).

Thirdly, we have estimated the parameters of real-life oceanic frontal flows (Table 3) and supplied examples for the above regime classification and the stability analysis (Tables 4 and 7, respectively).

Finally, we note that results on *continuously* stratified geostrophic fronts (Tai and Niiler, 1985; Benilov 1993, 1994, 1995b,c) demonstrate that the two-layer model bears all main features of geostrophic dynamics and provides a good qualitative description of oceanic frontal flows.

Acknowledgements

This work was supported by the Bilateral Science and Technology Collaboration Program of the Australian Department of Industry, Technology and Commerce; the International Science Foundation (Grant No. MKJ300); and the Russian Foundation for Basic Research (Grant No. 17358).

We are grateful to Benoit Cushman-Roisin, Bruce Warren and Referee B for valuable remarks.

References

- Benilov, E. S., "Large-amplitude geostrophic dynamics: the two-layer model," *Geophys. Astrophys. Fluid Dynam.* **66**, 67–79 (1992a).
- Benilov, E. S., "A note on the stability of one-layer geostrophic fronts," *Geophys. Astrophys. Fluid Dynam.* **66**, 81–86 (1992b).
- Benilov, E. S., "Baroclinic instability of large-amplitude geostrophic flows," *J. Fluid Mech.* **251**, 501–514 (1993).
- Benilov, E. S., "Dynamics of large-amplitude geostrophic flows: the case of 'strong' beta-effect," *J. Fluid Mech.* **262**, 157–169 (1994).
- Benilov, E. S., "On the stability of large-amplitude geostrophic flows in a two-layer fluid: the case of 'strong' beta-effect," *J. Fluid Mech.* **284**, 137–158 (1995a).
- Benilov, E. S., "Stability of large-amplitude geostrophic flows localized in a thin layer," *J. Fluid Mech.*, **288**, 157–174 (1995b).
- Benilov, E. S., "Baroclinic instability of a quasigeostrophic flow localized in a thin layer," *J. Fluid Mech.* **288**, 175–199 (1995c).
- Benilov, E. S. and Cushman-Roisin, B., "On the stability of two-layered large-amplitude geostrophic flows with thin upper layer," *Geophys. Astrophys. Fluid Dynam.* **76**, 29–41 (1994).
- Cushman-Roisin, B., "Frontal geostrophic dynamics," *J. Phys. Oceanogr.* **16** 132–143 (1986).